Transmission Expansion Planning for Renewable-energy-dominated Power Grids Considering Climate Impact

Jin Lu, *Student Member*, *IEEE* and Xingpeng Li, *Senior Member*, *IEEE*

***Abstract*—As renewable energy is becoming the major resource in future power grids, the weather and climate can have a higher impact on grid reliability. Transmission expansion planning (TEP) has the potential to reinforce the power transfer capability of a transmission network for climate-impacted power grids. In this paper, we propose a systematic TEP procedure for renewable-energy-dominated power grids considering climate impact (CI). Particularly, this paper develops an improved model for TEP considering climate impact (TEP-CI) and evaluates the reliability of power grid with the obtained transmission investment plan. Firstly, we create climate-impacted spatio-temporal future power grid data to facilitate the study of TEP-CI, which include the future climate-dependent renewable power generation as well as the dynamic line rating profiles of the Texas 123-bus backbone transmission (TX-123BT) system. Secondly, the TEP-CI model is proposed, which considers the variation in renewable power generation and dynamic line rating, and the investment plan for future TX-123BT system is obtained. Thirdly, a customized security-constrained unit commitment (SCUC) is presented specifically for climate-impacted power grids. The reliability of future power grid in various investment scenarios is analyzed based on the daily operation conditions from SCUC simulations. The whole procedure presented in this paper enables numerical studies on power grid planning considering climate impact. It can also serve as a benchmark for other studies of the TEP-CI model and its performance evaluation.**

***Index Terms*—Generation investment, power grid, renewable energy, reliability, climate, transmission expansion planning.**

NOMENCLATURE

A. Sets

B	Set of buses in power grid
D^T	Set of typical days in a year
$D^{T(D)}$	Set of typical weekdays in a year
$D^{T(E)}$	Set of typical weekends in a year
G	Set of existing generators in power grid
$G(p)$	Set of online generators in future period p
G'	Set of new generators in power grid
$G^{B(n)}$	Set of generators located on bus n
$G^{N,B(n)}$	Set of new generators located on bus n
$G(p)$	Set of generators including operating new generators in future period p
$K(n+)$, $K(n-)$,	Sets of lines that connect bus n with bus n being to-bus and from-bus
L	Set of transmission lines in power grid
L'	Set of candidate new lines
$L^{T(n)}$	Set of transmission lines, of which the to-bus is n
$L^{F(n)}$	Set of transmission lines, of which the from-bus is n
$L^{N,T(n)}$	Set of candidate new lines, of which the to-bus is n
$L^{N,F(n)}$	Set of candidate new lines, of which the from-bus is n
P	Set of future time periods studied in transmission expansion planning (TEP)
R	Set of renewable power plants in power grid
R'	Set of new renewable power plants in future power grid
$R^{B(n)}$	Set of renewable energy sources located on bus n
ST^1	Set of buses and time periods where available renewable power at bus is less than load demand
ST^2	Set of buses and time periods where available renewable power at bus exceeds load demand
T	Set of time intervals in a day

B. Parameters

C_g^G	Operation cost of generator g per MWh output
$C_g^{G'}$	Operation cost of new generator g per MWh output
C_g^{On}	Online cost of generator g
C_g^{SU}	Start-up cost of generator g

Manuscript received: December 15, 2023; revised: March 22, 2024; accepted: June 26, 2024. Date of CrossCheck: June 26, 2024. Date of online publication: August 7, 2024.

This paper was supported by the Alfred P. Sloan Foundation. We extend our gratitude to Dr. H. Li and his team for providing clean climate data, and to Dr. E. Yang and his team for providing ABM-based future generation investment data.

J. Lu and X. Li (corresponding author) are with the Department of Electrical and Computer Engineering, University of Houston, Houston, TX, 77204, USA (e-mail: jlu28@uh.edu; xingpeng.li@asu.edu).

DOI: 10.35833/MPCE.2023.000990

$C_k^{L'}$ Construction cost of line k

M A large number

N^P Number of periods in TEP study

N^Y Number of years in each future period

N^T Number of typical days in each year

N^D Number of weekdays in a quarter

N^E Number of weekends in a quarter

N^B Number of buses in power grid

$N_{p,d,n}^H$ Number of shedding hours on bus n in typical day d in future period p

$p_g^{\min}$ The minimum output power for generator g

$p_g^{\max}$ The maximum output power for generator g

$p_{g,p}^{\min}$ The minimum output power limit for new generator g in future period p

$p_{g,p}^{\max}$ The maximum output power limit for new generator g in future period p

$p_r^{\min,R}$ The minimum output power for renewable power plant r

$p_{r,t,d,p}^{\max,R}$ Available power output for renewable power plant r at time interval t in typical day d in future period p

$p_r^{\min,R'}$ The minimum output power for new renewable power plant r

$p_{r,t,d,p}^{\max,R'}$ Available power output for new renewable power plant r at time interval t in typical day d in future period p

$p_{k,t}^{\max}$ Active power rating of line k at time interval t

$p_{k,t,d,p}^{\max}$ Active power rating of line k at time interval t in typical day d in future period p

$p_{k,t,d,p}^{\max,L'}$ Active power rating of candidate new line k at time interval t in typical day d in future period p

$p_{p,d,n,t}$ Load on bus n at time interval t in typical day d in future period p

$p_{p,d,n,t}^S$ Load shedding of bus n at time interval t in typical day d in future period p

$p_{n,t,d,p}^D$ Load demand on bus n at time interval t in typical day d in future period p

$p_{n,t}^D$ Load demand on bus n at time interval t

$p_{r,t}^R$ Output power of renewable power plant r at time interval t

R_g^{10} Reserve ramping rate of generator g in 10 min

R_g Ramping rate of generator g

R^M Ratio of maintenance cost to construction cost of a transmission line

S^A Reference value of apparent power used for normalizing power quantities in per-unit system calculations

v^{10} Wind speed at 10 m height

v^{80} Wind speed at 80 m height

$x_k^{L'}$ Reactance of candidate new line k

z_0 Surface roughness length for wind power generation calculation

C. Variables

$\theta_{k,t}$ Phase angle difference of two terminal buses of line k at time interval t

$\theta_{k,t,d,p}^F$ Phase angle at from-bus of line k at time interval t in typical day d in future period p

$\theta_{k,t,d,p}^T$ Phase angle at to-bus of line k at time interval t in typical day d in future period p

C^{OP} Total operation cost of power grid in future periods

C^{CAP} Total capital cost of power grid in future periods

$p_{g,t,d,p}^G$ Active power output of generator g at time interval t in typical day d in future period p

$p_{g,t,d,p}^{G'}$ Active power output of new generator g at time interval t in typical day d in future period p

$p_{j,t,d,p}^L$ Active power flow on line j at time interval t in typical day d in future period p

$p_{j,t,d,p}^{L'}$ Active power flow on new line j at time interval t in typical day d in future period p

$p_{r,t,d,p}^R$ Active power output of renewable power plant r at time interval t in typical day d in future period p

$p_{r,t,d,p}^{R'}$ Active power output of new renewable power plant r at time interval t in typical day d in future period p

$p_{n,t}^S$ Load shedding on bus n at time interval t

$p_{n,t}^{RC}$ Renewable curtailment on bus n at time interval t

$p_{g,t}$ Output power of generator g at time interval t

$p_{k,t}$ Active power flow on line k at time interval t

$r_{g,t}$ Reserve of generator g at time interval t

$u_{g,t}^G$ Binary variable equal to 1 when generator g is online at time interval t and 0 otherwise

$u_{k,p}^{L'}$ Binary variable equal to 1 when candidate new line k is operating in future period p and 0 otherwise

$v_{g,t}^G$ Binary variable equal to 1 when generator g transitions from offline to online at time interval t and 0 otherwise

$v_{k,p}^{L'}$ Binary variable equal to 1 when candidate new line k is constructed in future period p and 0 otherwise

I. Introduction

DURING the operation of modern power grid, various economic and technical factors are considered to achieve both cost efficiency and physical reliability [1]-[3]. Economic dispatch and unit commitment minimize the total generation cost while considering the power flows, generator

production limits, and other constraints [4]-[6]. They rely on the collection or prediction of various data such as load demand, renewable power generation, and transmission network status [7]-[10]. Power grids need to be expanded to accommodate the rising demands and possess the necessary transmission capability for reliable operation. New investments or upgrades in transmission and generation need to be well planned to maintain the reliability of the power grids. The transmission expansion planning (TEP) typically looks several decades ahead due to the long construction time of transmission lines and the necessity to account for long-term shifts in load demand and generation. Generally, the TEP considers multiple scenarios of the future power grids for the planning period, and the associated daily operation conditions in these scenarios are estimated and evaluated. Therefore, successful TEP relies on detailed and accurate predictions of load demand and generation of the future power grids at the nodal or facility level. The load demands are complicated and hard to be predicted precisely in the long term due to various factors including weather and climate, socio-economics, and electrification in transportation and other industry sectors [11], [12]. The generation expansion including the locations and new types of generation is often a prerequisite for TEP. However, predicting the future generation investments at facility level is also complicated. Taking the U.S. as an example, different entities usually make their own decisions for developing new power plants [13]. After determining the generation expansion plan, the prediction of future renewable generation is also essential for a comprehensive TEP study on a renewable-energy-dominated power grid [14].

The planning horizon for TEP usually spans decades, and it is widely acknowledged that climate changes will be more pronounced compared with long-standing historical patterns [15], [16]. Climate changes can affect multiple sectors of the future power grids including load demand, generation, and transmission [17]-[19]. While the modern power grids are becoming cleaner and greener, renewable power generation is highly dependent on the environmental variables such as wind speed, solar radiation, and temperature, which may be affected by climate change. Besides, the load demands, especially those for heating, ventilation, and air conditioning, are highly correlated with the temperature [20]. Climate change may affect both the peak load demand and the average load demand. Moreover, the transfer capability of transmission line is influenced by weather conditions including temperature and wind. While the dynamic line rating (DLR) technique is becoming more widely adopted in the short-term operation of power grids, the impact of climate change on the transmission network should also be considered in the long-term planning. Based on the above-mentioned reasons, it is necessary to consider the climate impact on the TEP of future renewable-energy-dominated power grids.

The accurate and detailed profiles of future power grid are the foundation for TEP, and considering climate impact on various sectors of the power grid may make the power grid profiles closer to the actual conditions in the future. Hence, data preparation is very important for TEP. However, few studies are presented to create the future power grid profiles required for TEP. Most of the real-world power grid data are sensitive and not publicly accessible. Instead, many synthetic test cases are available for research purposes such as the IEEE/CIGRE benchmark cases [21], [22], the PEGASE test case [23], and the Polish Circle 2000 case [24]. Most of these cases represent the systems for a certain time snapshot only. While there are a handful of studies on the climate impact on power grids, very few studies present the spatio-temporal datasets of the future climate-impacted power grids which can be used by TEP. In this paper, we create the future profile of the Texas 123-bus backbone transmission (TX-123BT) system [25], which includes the renewable power generation and DLRs influenced by meteorological variables. The representative profiles are also created and used as different scenarios in TEP. The datasets can be used to study the operation, planning, resilience, and many other analyses on climate-impacted power grids. By utilizing this dataset, we are able to evaluate the performance improvement of TEP considering the climate impact.

The trend of decarbonization in the energy sector may lead to changes on both generation and demand sides. Due to incentive policies and other factors, more variable renewable energy (VRE) will be invested and deployed into the future power grid. Meanwhile, conventional generation such as coal and gas plants is expected to decline. According to the National Renewable Energy Laboratory, 70% of U.S. total energy is expected to be generated by renewable energies by 2035, and it will rise to 90% by 2050 [26]. Expected high penetration of renewable energies requires the improvement of current TEP strategies to handle the versatility and uncertainties of VRE. Therefore, the U.S. Department of Energy (DOE) is proposing the state-of-the-art TEP techniques to address challenges arising from high penetration of renewable energies [27]. Besides, climate change will directly influence the weather conditions in future, and thus inpact the renewable power generation. The impact may also increase the versatility and uncertainties of VRE, and thus increase the difficulties in operation and planning of future power grids. An intuitive method to adapt to the versatility is to increase the resolution of VRE in the TEP model. A model for TEP considering climate impact (TEP-CI) with higher resolution for renewable energy generation and line flow limits is proposed in this paper. With the TEP-CI model, an initial study can be conducted on the TEP-CI of renewable-energy-dominated power grids. It can also serve as a benchmark for developing more comprehensive TEP-CI models.

To numerically evaluate the performance of the TEP-CI model, we have developed a security-constrained unit commitment (SCUC) model that can reflect the impacts of future power grid investment and climate changes, and can be used to simulate the daily operations of future power grids. The SCUC simulations are conducted in all typical days to obtain the operation conditions of future power grids in different planning epochs. Three widely-used reliability indices, i.e., loss of load probability (LOLP), loss of load expectation (LOLE), and expected unserved energy (EUE), are used to evaluate the overall reliability of the power grid for each cer-

tain future period. We showcase how different types of investment will influence future power grid by conducting the reliability analysis in the following three cases, respectively: ① a power grid without any asset investment, referred as future (FR) case; ② a power grid with only future generation investment (FGI); and ③ a power grid with both future generation and transmission investment (FGTI). The reliability of future power grid under different investment situations is analyzed.

In the literature, very few studies address the creation of accurate future power grid profiles, or perform numerical analysis of the climate impact on the renewable-energy-dominated power grids, and how it will influence the TEP. In [28], the climate impact on various components of power system is discussed and concluded; however, no numerical analysis is conducted. In [29], the future planning of the climate-impacted Indonesian power grid is studied, which, however, consists of less than 20% renewable energy sources, and the climate impact is not considered. In [30], the climate impact on the generation mix of Portuguese power grids is studied. Since the generation is not studied at facility level, the study cannot capture the spatio-temporal characteristics of climate impact on renewable power generation.

Many studies focus on the modeling of transmission expansion considering the specific impact of weather or climate conditions. In [31], the stochastic TEP model includes the dynamic and uncertain nature of DLRs. The economic benefits obtained by considering the DLR are validated, but the reliability of the future power grids with its obtained investments are not investigated. A three-stage robust model that considers the climate impact on renewable power generation is proposed in [32]. The model accounts for the effects of El Niño and La Niña on renewable power generation but may not fully capture the nuances of climate impact on a regional scale. The model in [33] addresses the uncertainties of renewable power generation. However, it does not consider climate impact on renewable power generation and transmission line capacity.

Based on the above literature, current TEP utilizes the predicted information of future representative scenarios without considering the climate impact. Existing models do not consider higher temporal resolution and capture temporal changes for these power grid conditions. Existing evaluation of TEP focuses on economic aspects. The reliability of the future power grid, especially after suitable transmission investment, remains to be investigated. Few studies conclude and present the whole procedures of TEP, including data preparation, model formulation, and numerical evaluation. This paper addresses the climate impact on all these procedures. Various meteorological variables are considered in future renewable power generation and DLR profiles. The proposed TEP-CI model considers the fluctuation of weather-dependent renewable power generation and DLR. A specialized SCUC model which incorporates climate-dependent variations and load shedding is also required to obtain the daily operation conditions of future power grid for the reliability evaluations. The reliability indices which can evaluate power grid reliability for a long period in the future are calculated and compared. We evaluate the reliability of power grid with the proposed TEP-CI model to study the necessity and performance improvement after considering climate impact. The main contributions of this paper are summarized as below.

1) The climate-impacted profiles of the TX-123BT system from 2020 to 2050 including renewable power generation and DLRs are created. The representative profiles are also created for the planning and other scenario-based studies.

2) The TEP-CI model considers the versatility of renewable energy sources and climate impact, and is improved to adapt the spatio-temporal data of the representative profiles.

3) Three reliability indices, i.e., LOLP, LOLE, and EUE, are introduced to evaluate the long-term power grid reliability under various investment situations and TEP models.

The rest of this paper is structured as follows. Section II presents the procedures to create the time-sequential climate-impacted power grid profiles. Section III shows the TEP-CI model for renewable-energy-dominated power grids. The SCUC for TEP performance evaluation is presented in Section IV, while the reliability evaluation results are shown in Section V. The conclusions are drawn in Section VI.

II. Time-sequential Climate-impacted Power Grid Profiles

Typically, the TEP needs to consider the operation conditions of future power grid in different scenarios. Thus, the future power grid profiles including predicted load and generation information are critical for TEP to obtain a suitable transmission investment plan. The TEP requires both comprehensive technical data of the current grid configurations and future prospective information. The proposed TEP-CI model requires comprehensive geographic details of the power grid infrastructure and dependable prediction of future climate conditions specific to the region to create future power grid profiles that incorporate climate impacts.

The TX-123BT system is a synthetic power grid based on the footprint of Texas [34]. It is designed to represent the Electric Reliability Council of Texas (ERCOT) system, which covers most areas in Texas territory. It includes 345 kV high-voltage backbone transmission network distributed in ERCOT, which is shown in Fig. 1. The generator capacities and load distributions of the TX-123BT system are closely aligned with the actual ERCOT system as it was in 2019. Compared with other publicly accessible test power grids, TX-123BT system provides the geographic locations of all substations, transmission lines, thermal generators, and renewable power plants. These geographic locations are necessary to obtain the future climate and weather conditions at the facilities, which are required for the creation of renewable power generation and DLR profiles. We create the climate-impacted power grid profiles based on the future climate data extracted from Coupled Model Intercomparison Project Phase 6 (CMIP6) for 2020-2050. The CMIP6 is an advanced, comprehensive, coupled model global climate change project [35]. CMIP6 generates climate projections based on a variety of scenarios using complex climate models. The projections are based on a range of scenarios called shared socioeconomic pathways (SSPs) combined with representative concentration pathways (RCPs). SSPs describe possible future changes in demographics, economics, technolo-

gy, energy consumption, and land use. RCPs outline pathways of greenhouse gas concentrations and their radiative forcing on the climate system. By combining SSPs with RCPs, CMIP6 explores a wide range of future climate outcomes. The extracted data are for meteorological variables such as wind speed, solar radiation, and temperature under RCP 8.5, which is considered as the most likely global warming conditions if the world makes usual efforts on reducing the emission in the future [36]. We compare the predicted climate data from CMIP6 with the historical climate data from North American Land Data Assimilation System (NLDAS-2) [37] for the same period of 2019-2022, and verify that these meteorological variables in CMIP6 is coherent with the historical observations.

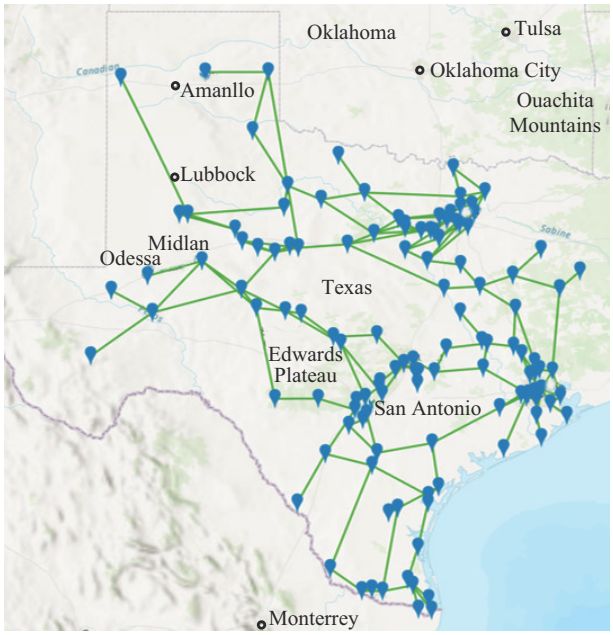

Fig. 1. High-voltage backbone transmission network of TX-123BT system.

Figure 2 displays a year-long comparison of temperature data in CMIP6 and NLDAS-2 at a bus location.

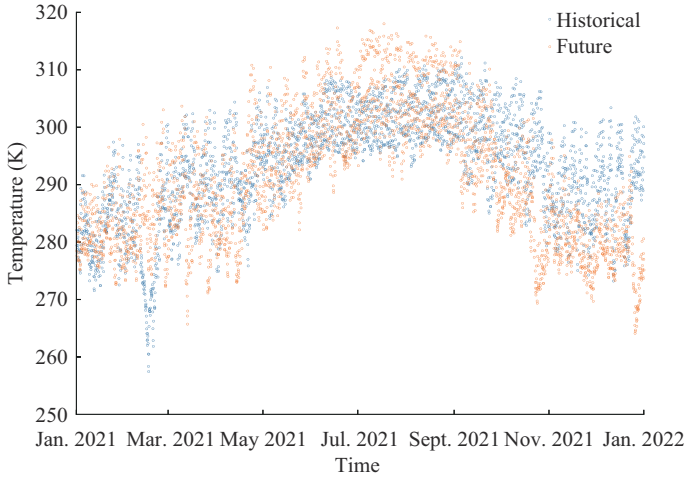

Fig. 2. Year-long comparison of temperature data in CMIP6 and NLDAS-2.

The CMIP6 climate data has three-hour resolution. In each three-hour period, the wind speed, solar radiation, and temperature data for all bus locations in TX-123BT system are extracted. Based on the weather-dependent models for DLR, solar and wind power generations in [34], the corresponding profiles are created for 2019-2050, and have the same three-hour resolution. The renewable power generation and DLR profiles are calculated for each renewable power plant or transmission line at three-hour resolution based on the future climate prediction at the specific location of the facility.

For DLR, the lower wind speed, higher temperature, and solar radiation on the two terminal buses of the transmission line are averaged, respectively, and then used in the calculation. The monthly average DLR at a transmission line (named as transmission line 1) for 2019-2024 is shown in Fig. 3.

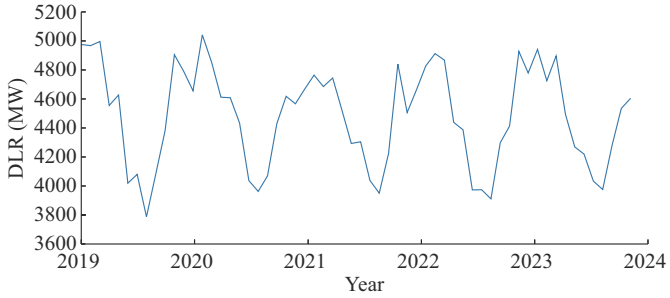

Fig. 3. Plot of monthly average DLR at transmission line 1.

The gross power output of a wind farm is the aggregation of all the wind turbines inside. To simplify the relationship between the wind speed at the wind farm location and the power output, we assume that the wind turbines in one wind farm are of the same type. Besides, the wind speed at the wind turbine height is required for the calculation of wind power generation. Since the wind speed in CMIP6 is the wind speed on the "earth surface" at 10 m height, we estimate the wind speed at 80 m height using the logarithmic wind profile method [38], which assumes that the wind speed increases with altitude due to the decrease in surface drag. This method provides a reliable approximation of wind speed at the turbine hub height, which is essential for creating the wind power generation profile based on the CMIP6 dataset. The logarithmic relationship between wind speeds at 80 m and 10 m heights is:

$$v_{80} = v_{10} \frac{\ln \frac{80}{z_0}}{\ln \frac{10}{z_0}} \tag{1}$$

Based on the estimated wind speed and the wind power generation model, the wind power generation profiles are created. The monthly average wind power generation of a wind power plant (wind power plant 72) is plotted in Fig. 4.

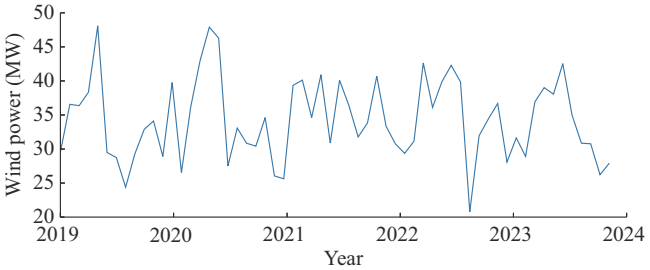

Fig. 4. Monthly average wind power generation of wind power plant 72.

The solar power generation is calculated using both shortwave and longwave radiation data extracted from CMIP6. The effective radiation on the solar panel is estimated based on the frequency range of the commonly used solar panels. The monthly average solar power generation of a solar power plant (solar power plant 66) is shown in Fig. 5. Due to the computation burden, planning models for future power grid such as TEP often consider a limited number of representative future scenarios. Hence, we create the representative daily profiles for every quarter of each five-year period from 2021 to 2050. Each representative profile encapsulates the average renewable power generation and DLRs derived from identical hours across all days within the same quarter. Since load demand is significantly affected by social activities, representative load demand profiles are established for weekdays and weekends within each quarter. The representative DLR, wind and solar power generations, and load demand profiles in 2021-2025 are shown in Fig. 6. In Fig. 6(a), the DLR in Quarter 1 is higher than other quarters due to the low temperature. In Quarter 3, the DLR is the lowest and drops obviously at noon time due to the high temperature. According to Fig. 6(b) and (c), the wind power generation is obviously lower in summer, while load is obviously higher. This illustrates why summer and winter (high wind power and low load power) scenarios are necessary to be both analyzed in some industrial applications in ERCOT.

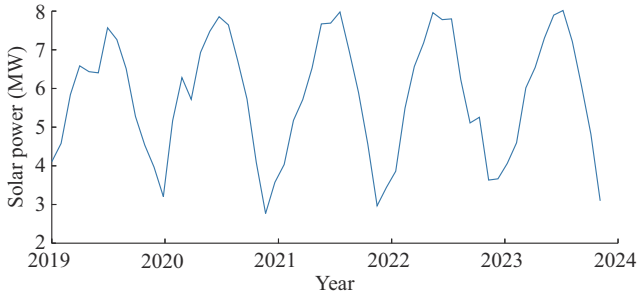

Fig. 5. Monthly averaged solar power generation of solar power plant 66.

Since the created representative profiles do not include the future newly invested power plants or transmission lines, they will be regarded as the benchmark case for the TEP simulation, referred to as the FR case in TX-123BT system. The new power plants including renewable energy sources are interconnected with the power grid through queue systems by various entities in the U.S.. An agent-based model (ABM) is used to mimic the generation investment behavior by market participators [39]. Each market participator is regarded as an agent and can make its own investment decisions based on the market and grid operation information. The ABM is selected due to its unique ability to model the complex interactions and decision-making processes among various stakeholders in the energy market including utility companies, independent power producers, and regulatory bodies. Unlike traditional models that might simplify these interactions through aggregated supply-demand curves or static investment decisions, ABM allows for a dynamic representation of how individual decisions and actions can lead to emergent market behaviors and investment patterns. In [39], the generation investment obtained from ABM is analyzed and validated. The future generation investment for TX-123BT system including the capacity and plant type of different market participants is obtained based on the ABM model. Then, the future generation of the new renewable resources is calculated. The future TX-123BT system with new generation investment and related profiles is named as the FGI case.

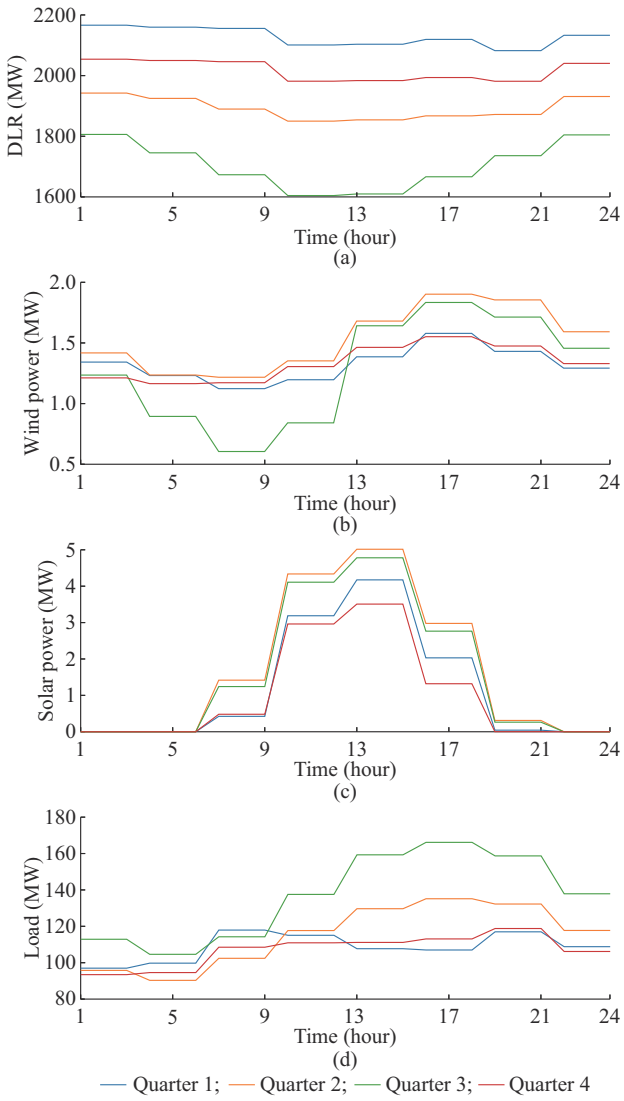

Fig. 6. Representative DLR, wind power generation, solar power generation, and load profiles in 2021-2025. (a) DLR of a line. (b) Wind power generation of a wind power plant. (c) Solar power generation of a solar power plant. (d) Load profiles on a bus.

III. TEP-CI Model for Renewable-Energy-Dominated Power Grids

Traditional TEP model considers the future power grid and market trends such as increasing load demands and fuel price, whereas the climate impact is not considered. The climate may impact the power grid on various sectors such as transmission, generation, and load demands. In Section II, the representative profiles including the renewable power generation and DLRs of the future climate-impacted power grid are created. In this paper, we address the timely chang-

ing characteristics of the renewable power generation and DLRs due to the meteorological variables in the TEP-CI model. In this section, the TEP-CI model and its transmission investment plan in the TX-123BT system are presented.

A. TEP-CI Model

In order to consider the components in TEP-CI model, we have made the following updates to the TEP model: ① the line flow capacity constraints now include the changing DLRs for different hours in the representative scenario; ② constraints are added to describe the available renewable energy sources in the power grid; and ③ the power balance equation is modified to include the weather-dependent renewable power generation and load profiles. After the update, the TEP-CI model can utilize the representative profiles created in Section II. The detailed TEP-CI model is shown below.

$$\min (C^{OP} + C^{CAP}) \tag{2}$$

$$C^{OP} = N^Y S^A \frac{365}{N^D} \sum_{g \in G, t \in T, d \in D^T, p \in P} p^G_{g,t,d,p} C^G_g + N^Y S^A \frac{365}{N^T} \sum_{g \in G', t \in T, d \in D^T, p \in P} p^{G'}_{g,t,d,p} C^{G'}_g \tag{3}$$

$$C^{CAP} = \sum_{k \in L', p \in P} V^{L'}_{k,p} C^{L'}_k [1 + (N^P - p + 1) R^M N^Y] \tag{4}$$

$$\sum_{j \in L^{T(n)}} p^L_{j,t,d,p} - \sum_{j \in L^{F(n)}} p^L_{j,t,d,p} + \sum_{j \in L^{N,T(n)}} p^{L'}_{j,t,d,p} - \sum_{j \in L^{N,F(n)}} p^{L'}_{j,t,d,p} + \sum_{g \in G^{B(n)}} p^G_{g,t,d,p} + \sum_{g \in G^{N,B(n)}} p^{G'}_{g,t,d,p} + \sum_{r \in R^{B(n)}} p^R_{r,t,d,p} + p^{R'}_{n,t,d,p} = p^D_{n,t,d,p} \quad \forall n \in B, t \in T, d \in D^T, p \in P \tag{5}$$

$$p^{\min}_g \le p^G_{g,t,d,p} \le p^{\max}_g \quad \forall g \in G, t \in T, d \in D^T, p \in P \tag{6}$$

$$p^{\min}_{g,p} \le p^{G'}_{g,t,d,y} \le p^{\max}_{g,p} \quad \forall g \in G', t \in T, d \in D^T, p \in P \tag{7}$$

$$p^{\min,R}_r \le p^R_{r,t,d,p} \le p^{\max,R}_{r,t,d,p} \quad \forall r \in R, t \in T, d \in D^T, p \in P \tag{8}$$

$$p^{\min,R'}_r \le p^{R'}_{r,t,d,y} \le p^{\max,R'}_{r,t,d,p} \quad \forall r \in R', t \in T, d \in D^T, p \in P \tag{9}$$

$$-p^{\max}_{k,t,d,p} \le p^L_{k,t,d,p} \le p^{\max}_{k,t,d,p} \quad \forall k \in L, t \in T, d \in D^T, p \in P \tag{10}$$

$$-M(1 - u^{L'}_{k,p}) \le p^{L'}_{k,t,d,p} - \frac{\theta^F_{k,t,d,p} - \theta^T_{k,t,d,p}}{x^{L'}_k} \le M(1 - u^{L'}_{k,p}) \quad \forall k \in L', t \in T, d \in D^T, p \in P \tag{11}$$

$$-p^{\max,L'}_{k,t,d,p} u^{L'}_{k,p} \le p^{L'}_{k,t,d,p} \le p^{\max,L'}_{k,t,d,p} u^{L'}_{k,p} \quad \forall k \in L', t \in T, d \in D^T, p \in P \tag{12}$$

$$\sum_{p' \in P, p' \le p} u^{L'}_{k,p'} \le u^{L'}_{k,p} \quad \forall k \in L', p \in P \tag{13}$$

$$v^{L'}_{k,p} \ge u^{L'}_{k,p} - u^{L'}_{k,p-1} \quad \forall k \in L', p \in P, p > 1 \tag{14}$$

$$v^{L'}_{k,1} = u^{L'}_{k,1} \quad \forall k \in L' \tag{15}$$

The TEP-CI model can minimize the operation and transmission investment cost for the studied period by (2). The operation cost includes both the existing and new thermal generators in (3). The capital cost of the transmission line is simplified by assuming that the yearly maintenance cost is part of the total construction cost in (4). The nodal power balance addresses the available renewable energy sources for each time interval by (5). The power output constraints for existing and newly invested thermal generators obtained from the ABM are described by (6) and (7), respectively. The renewable power generation output for each time interval should be under its available amount. To be noticed, $p^{\max,R}_{r,t,d,p}$ is the maximum available renewable output in the representative profiles, which is calculated using the CMIP6 climate data. The power output constraints for both existing and new renewable energy sources are (8) and (9), respectively. The line flow limit for existing transmission line is shown in (10), and $p^{\max}_{k,t,d,p}$ is the DLR in the representative profiles. To model the line flow limit of the new transmission line, we use a large number M and the binary variable $u^{L'}_{k,p}$ to enforce the DC power flow constraint when the line is constructed, as described in (11). The flow limit of the new lines is described by (12). And the constraints related to the binary variables for line construction are shown in (13)-(15).

While this model integrates a wide range of general physical constraints related to power flow and generators, it demands accurate prediction of future renewable power generation and DLRs affected by weather variations. The reliability of prediction hinges on specific climate models that may not encompass every potential future climate scenario, along with detailed geographic data at the facility level for the transmission network and renewable power plants.

B. Transmission Investment Plan of TEP-CI Model

TEP models are implemented using Python with Pyomo package [40]. Since the models are formulated as mixed-integer linear programming (MILP) problem, the commercial solver Gurobi [41] is used to find optimal solutions. The proposed TEP-CI model is designed to accommodate various resolution profiles such as one-hour or three-hour intervals, denoted by t periods within a day. Given that the profiles in this paper are created at a three-hour resolution, preserving this granularity in the model helps to shorten the simulation time without compromising the quality of solutions. In the first simulation of the TEP-CI model, we set the number of year-epoch to be three, and each epoch represents a five-year period. Thus, it determines the TEP of TX-123BT system in 2021-2035. Even for the FR case of TX-123BT system, which has no generation investments during this planning period, the TEP-CI model can easily find a feasible solution. The investment and system operation costs in 2021-2035 for FR case are presented in Table I. The new transmission line investment results are shown in Table II.

TABLE I
INVESTMENT AND SYSTEM OPERATION COSTS IN 2021-2035 FOR FR CASE

Cost type	Cost (billion $)
Generation cost	102.87
Transmission line investment cost	3.02
Total cost	105.89

The TEP-CI model finds 15 transmission lines to be invested. The transmission line investment cost is $3 million, which is about 2.94% of the total cost for the FR case of TX-123BT system in 2021-2035.

TABLE II
NEW TRANSMISSION LINE INVESTMENT RESULTS IN 2021-2035 FOR FR CASE

Line No.	Construction period	Line No.	Construction period	Line No.	Construction period
2	2021-2025	50	2025-2030	74	2026-2030
6	2026-2030	56	2025-2030	165	2026-2030
7	2021-2025	58	2025-2030	171	2026-2030
22	2025-2030	68	2025-2030	233	2031-2035
31	2021-2025	72	2021-2025	249	2021-2025

In the second simulation of the TEP-CI model, we set the number of year-epochs to be 6, which means that the TEP-CI model will give the transmission line investment results in 2021-2050. For this future period, the safe operation cannot be maintained without load shedding for FR case. The load demands are expected to increase rapidly in 2035-2050, and existing generation resources cannot meet the needs of such large amount of loads. Using the representative profiles under FGI case as input for the TEP-CI model, the simulation results are shown in Tables III and IV.

TABLE III
INVESTMENT AND SYSTEM OPERATION COSTS IN 2021-2050 FOR FGI CASE

Cost type	Cost (billion $)
Generation cost	146.76
Transmission line investment cost	6.00
Total cost	152.76

TABLE IV
NEW TRANSMISSION LINE INVESTMENT IN 2021-2050 FOR FGI CASE

Line No.	Construction period	Line No.	Construction period	Line No.	Construction period
3	2036-2040	49	2041-2045	83	2021-2025
6	2041-2045	57	2041-2045	112	2036-2040
7	2031-2035	72	2021-2025	147	2021-2025
8	2036-2040	80	2041-2045	189	2021-2025
9	2031-2035	74	2021-2025	191	2021-2025
30	2041-2045	82	2041-2045	247	2021-2025

The DLRs of the new transmission lines in the investment plan are calculated for the future periods after they are constructed. The new transmission lines and their DLR profiles are then integrated into the FGI case and form the future scenario that includes both generation and transmission investments, i.e., the FGTI case.

The comparisons between the proposed TEP-CI model and traditional TEP model [42] are concluded in Table V. For the results of the proposed TEP-CI model, the percentile value in the brackets indicates the increase or decrease compared with the results of the traditional TEP model. As observed from Table V, the proposed TEP-CI model results in higher transmission line investment costs due to its utilization of detailed and high-resolution climate-impacted profiles. While this model leads to higher initial transmission costs, it significantly lowers generation costs over the planning periods.

TABLE V
RESULTS OF PROPOSED TEP-CI AND TRADITIONAL TEP MODELS IN 2021-2035 FOR FGI CASE

Model	Total cost (billion $)	Transmission line investment cost (billion $)	Generation cost (billion $)	Total flow on transmission line (MWh)
Traditional TEP	79.34	0.24	79.1	18727
Proposed TEP-CI	55.73 (–29.7%)	0.47 (+95.8%)	55.26 (–30.1%)	22988 (+22.75%)

Table VI presents the solution time of the proposed TEP-CI model compared with traditional TEP model. For shorter planning spans such as 15 years, the solution time of the proposed TEP-CI model is not significantly extended. However, as the proposed TEP-CI model considers higher resolution of climate-impacted profiles, its solution time increases markedly for longer planning spans.

TABLE VI
SOLUTION TIME OF PROPOSED TEP-CI MODEL COMPARED WITH TRADITIONAL TEP MODEL

Planning span (year)	Solution time (s)	
	Traditional TEP model	Proposed TEP-CI model
15	209.5	214.7 (+2.48%)
30	6235.6	8821.1 (+41.4%)

In this paper, the simulations and results specifically for the TX-123BT system are presented. Adapting the proposed TEP-CI model to power grids across various geographic regions necessitates precise predictions for future renewable power generation and DLR profiles. Achieving accurate prediction of future renewable energy investments may involve the integration of region-specific climate and weather prediction data and utilization of ABM or other regionally appropriate methods.

IV. SCUC FOR TEP PERFORMANCE EVALUATION

The SCUC is modified and customized specifically for the future climate-impacted power grids and TEP performance evaluation. Firstly, to study the reliability performance of power grid under different investment plans, the load shedding should be considered in the SCUC. Specifically, the load shedding variables are introduced to the power balance equations, and the constraints describing the maximum shedding amount are added to the SCUC. The loads will be shedded only when the power grid cannot be operated safely. The shedding will happen when the physical constraints cannot be satisfied, because it may cause both economic losses and social disturbance. Hence, a penalty term is added to the objective function of the SCUC to make sure that the load shedding can only happen in time of need. With the proposed TEP-CI model, the SCUC solutions can give the information of the unserved load due to the increasing load de-

mand and climate change in the future.

Secondly, the power grid profiles have the same three-hour resolution as the climate data, while the commonly used SCUC has hourly resolution. We can simply transfer the three-hour resolution profiles into hourly profiles by assuming that the data during all the three hours are the same and used as hourly data input for SCUC. However, for both simulations of the SCUC on a large number of future profiles and the TEP for climate-impacted power grids, the number of time intervals will significantly influence the solution time. Hence, the SCUC is adjusted from hourly resolution to three-hour resolution. Besides, the SCUC input data such as generator costs c_0, c_1, and generator ramping rate are updated for three-hour resolution. The detailed formulation of SCUC for TEP evaluation is shown below.

$$\min \sum_{g\in G(p)}\sum_{t\in T}(C_g^G P_{g,t}+C_g^{On}u_{g,t}^G+C_g^{SU}v_{g,t}^G)+M\sum_{b\in B,t\in T}p_{n,t}^S \quad (16)$$

$$p_{n,t}^{RC}=0 \quad \forall (n,t)\in ST^1 \quad (17)$$

$$ST^1=\left\{(n,t)\,\middle|\, n\in B,t\in T,\ \text{s.t. } p_{n,t}^D-\sum_{r\in R(b)}p_{r,t}^R\ge 0\right\} \quad (18)$$

$$p_{n,t}^{RC}\le \sum_{r\in R(b)}p_{r,t}^R-p_{n,t}^D \quad \forall (n,t)\in ST^2 \quad (19)$$

$$ST^2=\left\{(n,t)\,\middle|\, n\in B,t\in T,\ \text{s.t. } p_{n,t}^D-\sum_{r\in R(n)}p_{r,t}^R<0\right\} \quad (20)$$

$$p_{n,t}^{RC}\le p_{n,t}^D-\sum_{r\in R(n)}p_{r,t}^R \quad \forall (n,t)\in ST^1 \quad (21)$$

$$p_{n,t}^{RC}=0 \quad \forall (n,t)\in ST^2 \quad (22)$$

$$P_g^{\min}u_{g,t}^G\le P_{g,t} \quad \forall g,\forall t \quad (23)$$

$$P_{g,t}+r_{g,t}\le P_g^{\max}u_{g,t} \quad \forall g,\forall t \quad (24)$$

$$0\le r_{g,t}\le R_g^{10}u_{g,t} \quad \forall g,\forall t \quad (25)$$

$$\sum_{m\in G}r_{m,t}\ge P_{g,t}+r_{g,t} \quad \forall g,\forall t \quad (26)$$

$$-R_g\le P_{g,t}-P_{g,t-1}\le R_g \quad \forall g,\forall t \quad (27)$$

$$P_{k,t}=\theta_{k,t}/x_k \quad \forall k,\forall t \quad (28)$$

$$-P_{k,t}^{\max}\le P_{k,t}\le P_{k,t}^{\max} \quad \forall k,\forall t \quad (29)$$

$$\sum_{g\in G(n)}P_{g,t}+\sum_{k\in K(n-)}P_{k,t}-\sum_{k\in K(n+)}P_{k,t}+\sum_{r\in R(n)}p_{r,t}^R=p_{n,t}^D+p_{n,t}^{RC}-p_{n,t}^S \quad \forall n,\forall t \quad (30)$$

$$v_{g,t}^G\ge u_{g,t}-u_{g,t-1} \quad \forall g,t>1 \quad (31)$$

In (16), the SCUC will optimize the operation cost for the day, and an additional term is added to ensure that the load shedding is employed strictly as a last resort. There will be no renewable power curtailment on a bus when the total renewable power is less than the load at the location according to (17) and (18). The maximum renewable power curtailment is constrained by (19) and (20). Similarly, the load shedding can only be made when the renewable power on the bus is not sufficient in (21) and (22). The minimum and maximum power outputs of thermal generator, the reserve constraints, and ramping limits are given in (23)-(27). The DC power flow and line flow limits are given in (28) and (29). The nodal power balance equation includes both the load shedding and renewable power curtailment by (30). The online and starting binary variables of generator are constrained in (31).

In each of the FR, FGI, and FGTI cases, the future representative profiles in 2021-2050 include 48 daily profiles for weekdays and weekends in each quarter with 5-year planning epoch. The SCUC simulations are run on all the daily profiles for different cases. The weekday highest load shedding for different quarters in FR case in 2041-2045 and 2046-2050 are shown in Fig. 7.

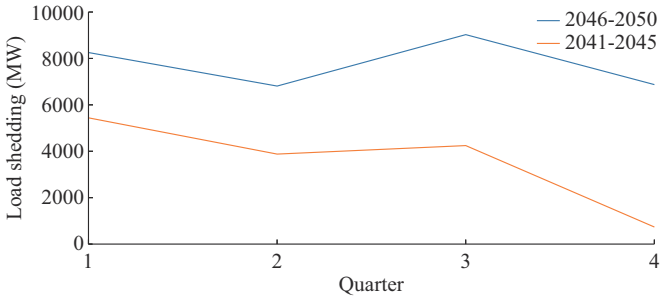

Fig. 7. Weekday highest load shedding for different quarters in FR case.

It can be observed that in the FR case, the power grid must necessarily shed loads after 2040. The required load shedding amount grows rapidly due to the increasing load demand. It indicates that the current power grid conditions cannot handle the increasing loads 20 years later. This is reasonable given the absence of expansion and development in generation and transmission infrastructure in FR case.

The weekend load shedding for Quarter 3 in FR case in 2041-2045 and 2046-2050 is plotted in Fig. 8. Load shedding in 2046-2050 is substantially greater than that in 2041-2045, and the daily shedding patterns differ significantly between the two 5-year spans.

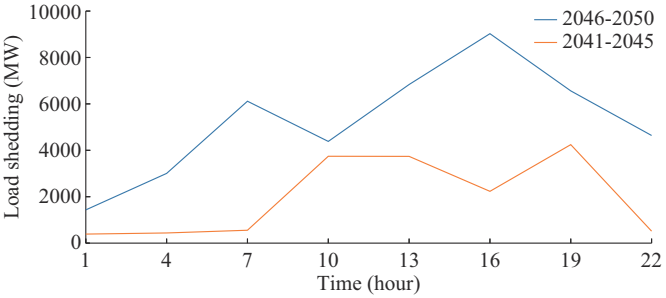

Fig. 8. Weekend load shedding for Quarter 3 in FR case.

In the FGTI case, Table VII summarizes the total operation cost and generation of thermal plants in Quarter 3 in FGTI case for different 5-year periods. A comparison between the weekdays in 2021-2025 and 2046-2050 reveals that the total generation has approximately doubled, while the total operation cost has roughly tripled. This discrepancy is attributable to the higher marginal prices associated with the high power output of generator. This situation arises be-

cause few thermal power plants are invested in the future, while the total generation is increasing.

TABLE VII
TOTAL OPERATION COST AND GENERATION OF THERMAL PLANTS IN QUARTER 3 IN FGTI CASE FOR DIFFERENT 5-YEAR PERIODS

5-year period	Total operation cost (M$)		Total generation (GWh)	
	Weekday	Weekend	Weekday	Weekend
2021-2025	11.55	11.62	711.1	714.2
2026-2030	13.94	13.90	810.3	808.6
2031-2035	17.41	15.31	940.3	858.5
2036-2040	21.52	17.90	1090.7	956.4
2041-2045	26.83	21.18	1263.9	1070.2
2046-2050	33.43	25.17	1462.1	1199.1

V. RELIABILITY EVALUATION RESULTS

To evaluate the reliability of future power grids in different cases, we develop several reliability indices which can be calculated based on the SCUC simulation results of the operation conditions for all days in the future. We select the concepts of reliability indices which are widely used in industry and academics. These indices include the EUE, LOLP, and LOLE. The three indices are the implications of the ability of the power grid to reliably meet the load demand from different aspects. Each index offers a unique lens through which the robustness and resilience of the power grid can be assessed, catering to the intricate dynamics of power supply and load demand. EUE quantifies the total energy that cannot be supplied due to power grid limitations within a specified time frame, serving as a direct measure of the magnitude of energy deficit. A higher EUE indicates more significant instances where the power grid fails to meet load demand, pointing towards potential weaknesses in generation capacity or transmission infrastructure. This index is especially crucial in evaluating the performance of power grid during peak load periods or in scenarios with high renewable energy variability, where the balance between supply and demand is most delicate. LOLP assesses the likelihood that the power grid will not meet the load demand at any given time, essentially reflecting the overall reliability of power grid. An increase in LOLP suggests a higher risk of power shortages, signaling the need for enhanced planning and investment. It underscores the importance of having sufficient reserve margins and flexible resources that can quickly respond to fluctuations in supply and demand. LOLE, expressed in hours per year, estimates the expected duration of load not being served. It complements LOLP by providing insight into the length of time when the power grid might be under stress, thus affecting consumer experience and economic activities. A lower LOLE value indicates that, while it may occasionally fail to meet the load demand, the power grid does so for the minimal duration of disruption to end-users.

In synthesizing the insights derived from EUE, LOLP, and LOLE, decision-makers and stakeholders gain a comprehensive understanding of the operation challenges of the power grid and the areas that require attention.

The EUE is an index that can evaluate the amount of total unserved energy for a given period such as one year. It can evaluate the scale of the outage by calculating the total amount of unserved energy.

$$EUE = \sum_{\substack{p\in P, d\in D^{T(D)},\\ n\in B, t\in T}} p^{S}_{p,d,n,t} N^{D} + \sum_{\substack{p\in P, d\in D^{T(E)},\\ n\in B, t\in T}} p^{S}_{p,d,n,t} N^{E} \tag{32}$$

The LOLP is the occurrence probability of load loss/shedding. Specifically, it measures how often the power grid cannot serve all loads such as load curtailment or blackout. The LOLP is usually calculated for a specific period such as one year.

$$LOLP = EUE \cdot \left(\sum_{\substack{p\in P, d\in D^{T(D)},\\ n\in B, t\in T}} p_{p,d,n,t} N^{D} + \sum_{\substack{p\in P, d\in D^{T(E)},\\ n\in B, t\in T}} p_{p,d,n,t} N^{E} \right)^{-1} \tag{33}$$

The LOLE can indicate the expected total outage duration for a specific period such as one year. In the LOLE calculation, we calculate the average outage hour on a bus for the entire year. Compared with LOLP, the LOLE can give us an insight on how long the load loss will last, instead of the occurrence probability of the load loss. As a brief conclusion, the LOLP, LOLE, and EUE can comprehensively evaluate the occurrence probability, duration, and the scale of load loss.

$$LOLE = \frac{1}{N^{B}} \left(\sum_{\substack{p\in P, d\in D^{T(D)},\\ n\in B}} N^{H}_{p,d,n} N^{D} + \sum_{\substack{p\in P, d\in D^{T(E)},\\ n\in B}} N^{H}_{p,d,n} N^{E} \right) \tag{34}$$

The results of different risk indices of future TX-123BT system without investment, with the proposed TEP-CI model, and with traditional TEP model and generation investment are shown in Tables VIII-X, respectively. With the transmission line investments planned by the TEP-CI model, all three reliability indices for 2041-2045 decrease significantly. For the period 2046-2050, the LOLP and EUE are both reduced significantly due to the transmission investments. LOLE has not decreased as substantially as the other two indicators, which suggests that while the severity of outages has been significantly mitigated, their time durations remain prolonged. Based on the results and analysis, the reliability of future power grid is remarkably improved with the transmission investments obtained by the proposed TEP-CI model.

TABLE VIII
DIFFERENT RISK INDICES OF FUTURE TX-123BT SYSTEM WITHOUT INVESTMENT

5-year period	Annual LOLP (%)	LOLE (hour/bus)	EUE (MWh)
2021-2025	0	0	0
2026-2030	0	0	0
2031-2035	0	0	0
2036-2040	0.013	2.92 (0.036%)	69105
2041-2045	0.810	25.36 (0.320%)	4803316
2046-2050	4.060	125.26 (1.550%)	27233362

TABLE IX
DIFFERENT RISK INDICES OF FUTURE TX-123BT SYSTEM WITH PROPOSED TEP-CI MODEL

5-year period	Annual LOLP (%)	LOLE (hour/bus)	EUE (MWh)
2021-2025	0	0	0
2026-2030	0	0	0
2031-2035	0	0	0
2036-2040	0	0	0
2041-2045	0.0716	2.92 (0.036%)	380304
2046-2050	2.5600	100.48 (1.240%)	17148794

TABLE X
DIFFERENT RISK INDICES OF FUTURE TX-123BT SYSTEM WITH TRADITIONAL TEP MODEL AND GENERATION INVESTMENT

5-year period	Annual LOLP (%)	LOLE (hour/bus)	EUE (MWh)
2021-2025	0	0	0
2026-2030	0	0	0
2031-2035	0	0	0
2036-2040	0	0	0
2041-2045	0	0	0
2046-2050	0.0626	24.0 (0.29%)	419486

VI. CONCLUSION

As more weather-dependent renewable power generations are expected in future power grids, the improvement to the current TEP model is required. A systematic procedure including data preparation, model improvement, and reliability evaluation of the proposed TEP-CI model is presented in this paper.

To address the climate impact on the future power grid that will be considered in the TEP-CI model, the future weather-dependent spatio-temporal profiles for the TX-123BT system are created. The proposed TEP-CI model considers these representative profiles in each planning epoch. The SCUC simulations are conducted on the future power grids in different investment cases including FR, FGI, and FGTI. The reliability indices are proposed and calculated for each future planning epoch based on the daily operation conditions. The reliability of the power grid in FR, FGI, and FGTI cases are compared and analyzed. This paper depicts the scheme of the TEP considering climate impact and paves the way for further planning studies.

REFERENCES

[1] D. Kirschen and G. Strbac, *Fundamentals of Power System Economics*. Hoboken: Wiley, 2019.

[2] X. Li and K. W. Hedman, "Enhanced energy management system with corrective transmission switching strategy – part I: methodology," *IEEE Transactions on Power Systems*, vol. 34, no. 6, pp. 4490-4502, Nov. 2019.

[3] J. Zhu, *Optimization of Power System Operation*. New York: John Wiley & Sons, 2015.

[4] A. V. Ramesh and X. Li, "Spatio-temporal deep learning-assisted reduced security-constrained unit commitment," *IEEE Transactions on Power Systems*, vol. 39, no. 2, pp. 4735-4746, Sept. 2023.

[5] J. Su, P. Dehghanian, and M. A. Lejeune, "Price-based unit commitment with decision-dependent uncertainty in hourly demand," *IET Smart Grid*, vol. 5, no. 1, pp. 12-24, Feb. 2022.

[6] C. Zhao and X. Li, "An alternative method for solving security-constrained unit commitment with neural network based battery degradation model," in *Proceedings of 2022 North American Power Symposium (NAPS)*, Denver, USA, Oct. 2022, pp. 1-6.

[7] N. Kayastha, D. Niyato, E. Hossain *et al.*, "Smart grid sensor data collection, communication, and networking: a tutorial," *Wireless Communications and Mobile Computing*, vol. 14, no. 11, pp. 1055-1087, Jul. 2012.

[8] L. Coppolino, S. D'Antonio, I. A. Elia *et al.*, "Security analysis of smart grid data collection technologies," in *Proceedings of 30th International Conference on Computer Safety, Reliability, and Security*, Naples, Italy, Sept. 2011, pp. 143-156.

[9] K. Muralitharan, R. Sakthivel, and R. Vishnuvarthan, "Neural network based optimization approach for energy demand prediction in smart grid," *Neurocomputing*, vol. 273, pp. 199-208, Jan. 2018.

[10] F. Mirzapour, M. Lakzaei, G. Varamini *et al.*, "A new prediction model of battery and wind-solar output in hybrid power system," *Journal of Ambient Intelligence and Humanized Computing*, vol. 10, no. 1, pp. 77-87, Jan. 2017.

[11] M. S. Kandil, S. M. El-Debeiky, and N. E. Hasanien, "Long-term load forecasting for fast developing utility using a knowledge-based expert system," *IEEE Transactions on Power Systems*, vol. 17, no. 2, pp. 491-496, May 2002.

[12] J. Zhu, Z. Yang, M. Mourshed *et al.*, "Electric vehicle charging load forecasting: a comparative study of deep learning approaches," *Energies*, vol. 12, no. 14, p. 2692, Jul. 2019.

[13] Federal Energy Regulatory Commission (FERC). (2023, Dec.). FERC order 2003: initial pro forma large generator interconnection procedures (LGIP). [Online]. Available: https://ferc.gov/electric-transmission/generator-interconnection/final-rules-establishing-and-revising-standard

[14] A. Moreira, D. Pozo, A. Street *et al.*, "Reliable renewable generation and transmission expansion planning: co-optimizing system's resources for meeting renewable targets," *IEEE Transactions on Power Systems*, vol. 32, no. 4, pp. 3246-3257, Nov. 2017.

[15] Intergovernmental Panel on Climate Change (IPCC). (2021, Dec.). Climate change 2021: the physical science basis. [Online]. Available: https://report.ipcc.ch/ar6/wg1/IPCC_AR6_WGI_FullReport.pdf

[16] J. Hansen, M. Sato, R. Ruedy *et al*., "Global temperature change," *Proceedings of the National Academy of Sciences of the United States of America*, vol. 103, no. 39, pp. 14288-14293, Sept. 2006.

[17] M. Auffhammer, P. Baylis, and C. H. Hausman, "Climate change is projected to have severe impacts on the frequency and intensity of peak electricity demand across the United States," *Proceedings of the National Academy of Sciences of the United States of America*, vol. 114, no. 8, pp. 1886-1891, Feb. 2017.

[18] F. Qiu and J. Wang, "Distributionally robust congestion management with dynamic line ratings," *IEEE Transactions on Power Systems*, vol. 30, no. 4, pp. 2198-2199, Jul. 2015.

[19] M. A. Russo, D. Carvalho, N. Martins *et al*., "Forecasting the inevitable: a review on the impacts of climate change on renewable energy resources," *Sustainable Energy Technologies and Assessments*, vol. 52, p. 102283, May 2022.

[20] P. Dhanasekar, C. Zhao, and X. Li, "Quantitative analysis of demand response using thermostatically controlled loads," in *Proceedings of IEEE PES Innovative Smart Grid Technology (ISGT)*, New Orleans, USA, Apr. 2022, pp. 1-5.

[21] University of Washington. (2023, Nov.). 118 bus power flow test case. [Online]. Available: http://labs. ece. uw. edu/pstca/pf118/pg_tca118bus. htm

[22] CIGRE, "Long term dynamics phase II: final report," Tech. Rep., CIGRE Task Force 38-02-08, 1995.

[23] S. Fliscounakis, P. Panciatici, F. Capitanescu *et al.*, "Contingency ranking with respect to overloads in very large power systems taking into account uncertainty, preventive, and corrective actions," *IEEE Transactions on Power Systems*, vol. 28, no. 4, pp. 4909-4917, Mar. 2013.

[24] Matpower. (2023, Dec.). Description of case2383wp. [Online]. Available: https://matpower.org/docs/ref/matpower5.0/case2383wp.html

[25] J. Lu and X. Li. (2023, Mar.). Future profiles of Texas 123-bus backbone transmission (TX-123BT) system. [Online]. Available: https://figshare. com/articles/dataset/Future_Profiles_of_TX-123BT/22266991? file =39584908

[26] P. Gagnon. (2023, Jan.). 2022 standard scenarios report: a U.S. electricity sector outlook. [Online]. Available: https://www. nrel. gov/docs/fy23osti/84327.pdf

[27] U.S. Department of Energy. (2023, Oct.). Operation and planning tools for inverter-based resource management and availability for future power systems (optima). [Online]. Available: https://energycommunities. gov/funding-opportunity/operation-and-planning-tools-for-inverter-

based-resource-management-and-availability-for-future-power-systems-optima/
[28] M. T. Craig, S. Cohen, J. Macknick *et al*., "A review of the potential impacts of climate change on bulk power system planning and operations in the United States," *Renewable and Sustainable Energy Reviews*, vol. 98, pp. 255-267, Sept. 2018.
[29] K. Handayani, T. Filatova, Y. Krozer *et al*., "Seeking for a climate change mitigation and adaptation nexus: analysis of a long-term power system expansion," *Applied Energy*, vol. 262, p. 114485, Jan. 2020.
[30] J. N. Fidalgo, D. de Sao Jose, and C. Silva, "Impact of climate changes on the Portuguese energy generation mix," in *Proceedings of International Conference on European Electricity Market*, Ljubljana, Slovenia, Sept. 2019, pp. 1-6.
[31] J. Zhan, W. Liu, and C. Y. Chung, "Stochastic transmission expansion planning considering uncertain dynamic thermal rating of overhead lines," *IEEE Transactions on Power Systems*, vol. 34, no. 1, pp. 432-443, Jan. 2019.
[32] A. Moreira, D. Pozo, A. Street *et al.*, "Climate-aware generation and transmission expansion planning: a three-stage robust optimization approach," *European Journal of Operational Research*, vol. 295, no. 3, pp. 1099-1118, Dec. 2021.
[33] S. Lumbreras, A. Ramos, and F. Banez-Chicharro, "Optimal transmission network expansion planning in real-sized power systems with high renewable penetration," *Electric Power Systems Research*, vol. 149, pp. 76-88, Aug. 2017.
[34] J. Lu, X. Li, H. Li *et al.* (2023, Feb.). A synthetic Texas backbone power system with climate-dependent spatio-temporal correlated profiles. [Online]. Available: https://arxiv.org/abs/2302.13231
[35] Lawrence Livermore National Laboratory. (2023, Sept.). CMIP6 – coupled model intercomparison project phase 6. [Online]. Available: https://pcmdi.llnl.gov/CMIP6/
[36] K. Riahi, "RCP 8.5 – a scenario of comparatively high greenhouse gas emissions," *Climatic Change*, vol. 109, no. 1-2, pp. 33-57, Aug. 2011.
[37] NASA. (2023, Sept.). NLDAS-2 model data. [Online]. Available: https://ldas.gsfc.nasa.gov/nldas/nldas-2-model-data
[38] J. Holmes, P. Carol, and K. Robert, *Wind Loading of Structures*, Boca Raton: CRC Press, 2007.
[39] A. Ghaffari, F. Hung, J. Lu *et al*., "Development of a coupled agent-based generation expansion planning tool with a power dispatch model," *Energy and Climate Change*, vol. 5, p. 100156, Dec. 2024.
[40] Pyomo. (2024, Mar.). Pyomo package. [Online]. Available: http://www.pyomo.org/
[41] Gurobi. (2024, Mar.). Gurobi optimization solver. [Online]. Available: https://www.gurobi.com/
[42] X. Li and Q. Xia, "Transmission expansion planning with seasonal network optimization," in *Proceedings of 2020 IEEE PES Innovative Smart Grid Technologies Conference (ISGT)*, Washington D.C., USA, Feb. 2020, pp. 1-5.

Jin Lu received the B.S. degree in electrical engineering from Dalian Maritime University, Dalian, China, in 2019, and the M.S. degree in electrical engineering from the University of Houston, Houston, USA, in 2020. He is currently pursuing the Ph.D. degree in electrical engineering at the University of Houston. From 2020 to 2024, he was a Research Assistant with the Renewable Power Grid Lab at the University of Houston. His research interests include power system operation and planning, power system restoration, and renewable power system with hydrogen energy.

Xingpeng Li received the B.S. degree in electrical engineering from Shandong University, Jinan, China, in 2010, and the M.S. degree in electrical engineering from Zhejiang University, Hangzhou, China, in 2013. He received the M.S. degree in industrial engineering and the Ph.D. degree in electrical engineering from Arizona State University, Phoenix City, USA, in 2016 and 2017, respectively. He also received the M.S. degree in computer science from Georgia Institute of Technology, Atlanta, USA, in 2023. From 2017 to 2018, he was a Senior Application Engineer with ABB's power grid division (now Hitachi Energy), San Jose, USA. Since 2018, he has been an Assistant Professor with the Department of Electrical and Computer Engineering at the University of Houston, Houston, USA. His research interests include application of machine learning and optimization methods in power systems, power system control, operation and planning, grid integration of renewable generation, optimal sizing and energy management of microgrids, distributed energy resource, energy storage, and battery degradation.